Crustal loading in vertical GPS time series in Fennoscandia

Maaria Nordman, Jaakko Mäkinen, Heikki Virtanen, Jan M. Johansson, Mirjam Bilker-Koivula, Jenni Virtanen

Accepted Manuscript

Title: Crustal loading in vertical GPS time series in Fennoscandia

Authors: Maaria Nordman, Jaakko Mäkinen, Heikki Virtanen, Jan M. Johansson, Mirjam Bilker-Koivula, Jenni Virtanen

1 **Crustal loading in vertical GPS time series in Fennoscandia**

2

3 Maaria Nordman[*] (1), Jaakko Mäkinen (1), Heikki Virtanen (1), Jan M. Johansson

4 (2), Mirjam Bilker-Koivula (1), Jenni Virtanen (1)

5

6 1 Finnish Geodetic Institute, Geodeetinrinne 2, P.O. Box 15, 02431 Masala, Finland

7 2 Chalmers University of Technology, Onsala Space Observatory, Sweden.

8 * Corresponding author, Maaria.Nordman@fgi.fi, tel. +358 9 29555216, Fax +358 9

9 29555211

10

11 Abstract

12 We compare time series of vertical position from GPS with modelled vertical

13 deformation caused by variation in continental water storage, variation in the level of

14 the Baltic Sea, and variation in atmospheric pressure. Monthly time series are used.

15 The effect of continental water storage was calculated from three different global

16 models. The effect of non-tidal variation in Baltic Sea level was calculated using tide

17 gauge observations along the coasts. Atmospheric loading was computed from a

18 numerical weather model. The loading time series are then compared with three

19 different GPS time series at seven stations in Fennoscandia. A more detailed analysis

20 is computed at three coastal stations. When the monthly GPS time series are corrected

21 using the load models, their root-mean-square scatter shows an improvement between

22 40 and zero percent, depending on the site and on the GPS solution. The modelled

23 load effect shows a markedly seasonal pattern of 15 mm peak-to-peak, of which the

24 uncorrected GPS time series reproduce between 60 and zero percent.

25

1

27   **Introduction**

28   The geographical distribution of atmospheric, oceanic and hydrologic masses varies in

29   time and this in turn loads and deforms the surface of the solid Earth. Such

30   deformations can be detected by GPS. Height changes due to atmospheric loading

31   were pointed out in global time series of GPS coordinates by van Dam et al. (1994).

32   The deformation due to variable loading by continental water storage was found by

33   van Dam et al (2001). Blewitt et al. (2001) demonstrated that a global mode of

34   seasonal mass exchange between the Northern and Southern hemisphere is detectable

35   in GPS data.

36

37   Many of the mass fluxes that produce the deformation follow a near-annual cycle. In

38   fact, time series of GPS positions typically show a seasonal variation, which is

39   tempting to associate with geophysical loads. However, Dong et al. (2002) estimated

40   that only about 40% of the seasonal power of apparent vertical motion could be

41   attributed to modelled mass redistribution. Similarly, e.g. van Dam et al (2007) found

42   large discrepancies between seasonal vertical displacements estimated from GRACE

43   and observed at European GPS sites. The discrepancies are believed to be due to

44   technique errors and unmodelled or mismodelled factors in the GPS analysis.

45   Candidates for producing spurious long-period signals in the GPS time series include

46   the propagation of unmodelled short-period signals like tides to longer periods (Penna

47   and Stewart, 2003, Stewart et al., 2005, Penna et al., 2007, King et al. 2008),

48   mismodelling of troposphere delays (Munekane et al., 2008), the satellite repeat

2

49 constellation (Ray et al., 2008), monument movements, variation in local multipath

50 (Dong et al., 2002, Williams et al., 2004).

51

52 In this paper we investigate the agreement between GPS time series and independent

53 loading models in Fennoscandia, and the subsequent application of the models to

54 reducing GPS time series residuals. We compare time series of vertical positions from

55 GPS with modelled vertical deformation from three geophysical loads. They are the

56 atmospheric pressure variation, non-tidal variation in Baltic sea level, and continental

57 hydrology. The loads are studied at seven continuous GPS stations, five in Sweden,

58 one in Finland, and one in Norway (Figure 1a). We want to see whether the residuals

59 in the GPS time series can be reduced by the model corrections. We also compare the

60 seasonal pattern in GPS and in the load models. Our data on Baltic level is monthly,

61 as are the hydrology models. Therefore the GPS and atmospheric loading time series

62 are averaged to monthly means as well (see next chapter).

63 [Figure 1]

Data and methods

64

GPS

65

66 Figure 1a shows the positions of the 7 stations. We use three daily GPS time series of

67 vertical positions. Two of them are by M.B. Heflin and were obtained from the

68 Processing Centre of the International GNSS Service (IGS) at the Jet Propulsion

69 Laboratory (JPL) (http://sideshow.jpl.nasa.gov/mbh/series.html). These solutions

70 apply the no-fiducial strategy and GIPSY software. Daily solutions are aligned to the

71 ITRF2005 in the least-squares sense using either a 6-parameter (translation, rotation)

72 or 7-parameter (translation, rotation, scale) Helmert transformation. Hereafter we

3

73 refer to them as MHp6 and MHp7, respectively. The starting years for these time

74 series varies, from 1993 to 2004 depending on the station.

75

76 The third GPS time series is the one used for BIFROST studies (Johansson et al.,

77 2002). This is also calculated using the no-fiducial strategy and GIPSY. Satellite

78 orbits were referred to various releases of the International Terrestral Reference

79 Frame ITRF. The geodetic positions were then transformed to a frame provided by M.

80 Heflin, using a core subset of the BIFROST stations; for description see Johansson et

81 al. (2002). We refer to this time series as JJ and the data span is 1993–2006 at all our

82 stations.

83

84 All time series use the same strategy, cut-off angle of $15°$ and IERS conventions for

85 the solid Earth tide and ocean tidal loading. The models of ocean tidal loading used in

86 GPS processing do not include Baltic tides. They are a few centimetres only, and thus

87 negligible in the terms of the load. The effect of non-tidal ocean loading for our

88 stations is small, 1.5-2 mm peak-to-peak from the ECCO-model (Takiguchi et al.

89 2006), and is neglected. At the (seasonal) timescales of interest here, the GPS time

90 series approximately refer to the CF (Center of Figure) frame (Dong et al., 2002).

91

92 Since the GPS time series show larger scatter in the beginning, we left the first years

93 out and chose a time period 1997-2006 (10 years) for all the stations, when available.

94 All daily series were decimated to monthly series taking the simple average over a

95 calendar month. The time series of all the stations are plotted in Figure 1b.

4

96 *Baltic Sea*

97 We used monthly tide gauge (TG) data from all around the Baltic, provided by the

98 Permanent Service for Mean Sea Level (Woodworth and Player, 2003). The reference

99 for the sea level was determined by regression of the whole lengths of the TG records

100 and by fixing the epoch to 2000.5. Monthly series of a sea surface model were created

101 using the minimum-curvature-surface interpolation scheme with splines (Smith and

102 Wessel, 1990). The number of available TG stations varies monthly, between 22 and

103 26, but the interpolation scheme is not sensitive to missing support points. The

104 loading deformation was calculated from these sea-surface models by convolving

105 them with the Green's function from the Gutenberg-Bullen Earth model (Farrell,

106 1972). The degree one Love numbers applied by Farrell (1972) imply that the frame is

107 CE (Center of mass of the solid Earth). For our purposes, the difference from CF

108 frame is negligible (Dong et al., 2002). Steric effects were neglected, i.e. sea heights

109 were equated with sea mass. For more details see Virtanen et al. (2008). An example

110 of a monthly Baltic Sea load deformation can be seen in Figure 1a.

111 *Atmospheric loading*

112 We use the atmospheric pressure loading time series provided by the Goddard VLBI

113 group, available on the Web at http://gemini.gsfc.nasa.gov/aplo/. They were computed

114 by convolving the Green's function from the Preliminary Earth Model (PREM) with a

115 surface pressure field (Petrov and Boy, 2004). The surface pressure field comes from

116 the NCEP/NCAR Reanalysis numerical weather model and has a 2.5 x 2.5 degree

117 spatial resolution and 6-hour temporal resolution. We averaged the 6-hour values to

118 monthly means. In this time series, oceans are assumed to have the inverse barometer

119 (IB) response, but semi-enclosed seas like the Baltic Sea are taken to be "dry land",

5

120   which is consistent with the Baltic Sea load computation. The frame of the time series

121   is CM, i.e., Centre of Mass of the entire solid Earth plus load.

122   *Continental water storage*

123   We used three monthly models of continental water storage. The model of the Climate

124   Prediction Centre (CPC, Fan and van den Dool, 2004) only contains soil moisture, but

125   its leaky-bucket model can hold 0.76 m of water and therefore is capable of partly

126   accounting for groundwater, too. Snowfall is modelled as liquid water and thus it may

127   exit from the model too fast. The WaterGAP Global Hydrology Model (WGHM; Döll

128   et al. 2003) and the LaDWorld Gascoyne (Milly and Shmakin, 2002) account for all

129   aspects of water storage: snow, soil moisture, groundwater. We have used each model

130   in the whole area where it is released. WGHM excludes the polar ice sheets but

131   LaDWorld and CPC cover them.

132

133   To compensate for the change in total continental water storage, we add or subtract a

134   uniform layer of water to/from the oceans. Thus the global water mass is conserved

135   but gravitational consistency (Clarke et al., 2005) is not implemented. The time series

136   of deformation are then calculated by convolving the global loads with the Green's

137   function from the Gutenberg-Bullen Earth model by Farrell (1972). The frame is CE

138   (cf. the Baltic Sea above).

139   **Results and discussion**

140   *Time series plots*

141   In the following figures all loads are relative to a mean value and time series plots

142   have been detrended. An example of a monthly Baltic Sea load can be seen in

143   Figure 1a. The deformation decreases rapidly with growing distance from the sea.

6

144

145 Figure 2a shows the monthly time series at Metsähovi: GPS, loading, and GPS

146 residuals after removing all loads. Figures 2b, 2c and 2d show the same time series at

147 Kiruna, Mårtsbo and Onsala, but with Metsähovi subtracted. Obviously, at closeby

148 stations the loading signals are very similar. However, at longer distances clear

149 differences already emerge, e.g. in the hydrological loading between Kiruna and

150 Metsähovi. Noteworthy are also the relatively large discrepancies between the

151 different hydrological models. The plots for Borås (not shown) are rather similar to

152 Onsala and Tromsö (not shown) resembles Kiruna.

153

154 As we are particularly interested in loading by the Baltic Sea, we have chosen three

155 stations for closer analysis: Metsähovi, Mårtsbo, and Visby. At the other stations its

156 loading is small.

157 [Figure 2]

158 ***Load time series as corrections to GPS***

159 Here we look at the load time series as corrections to GPS. We have computed the

160 standard deviations of the three GPS time series before and after the load effects in

161 various combinations have been corrected for. The standard deviations of the

162 individual load effects are given, too. This is done for the Visby station in Table 1, for

163 Mårtsbo in Table 2, and for Metsähovi in Table 3. We have then calculated the

164 reduction in the standard deviation with respect to the original GPS time series. The

165 change is expressed in percent and is negative if the standard deviation decreases, i.e.

166 improves. Note that for Visby and Mårtsbo the GPS time series MHp6 and MHp7

167 have only three years of data and for comparison also three-year period has been

168 computed for JJ solution (JJS). All the other GPS time series cover the period January

7

169 1997 to December 2006. Tables 1, 2 and 3 show that the performance of the

170 corrections depends on the site and on the GPS time series in question, both on its

171 length and on the solution (JJ or MH).

172 [Table 1]

173 [Table 2]

174 [Table 3]

175 At Visby the Baltic Sea correction reduces the standard deviation in all time series, for

176 MH time series also the hydrology correction helps. For the three-year time series at

177 Mårtsbo the hydrology models and Baltic Sea correction reduce the standard deviation

178 using almost every combination, whereas the ten-year time series (JJ) for the same

179 stations hardly improve. At Metsähovi the highest reductions are achieved in MHp6

180 using hydrology correction only.

181

182 The ten-year series MHp7 and JJ at Metsähovi respond almost identically to the

183 corrections, similarly the three-year series MHp7 and JJS at Mårtsbo. In fact this

184 could be expected as the GPS time series themselves (Fig 1a) are very similar. At

185 Visby the three-year series MHp7 and JJS differ appreciably in the winter 2006

186 (Fig 1a) and so does their response to the load corrections.

187

188 In nearly all instances, the hydrological time series improve MHp7 less than they do

189 MHp6. The difference between the MHp6 and MHp7 is that in the latter series a scale

190 parameter is included in the alignment to ITRF2005. Possibly the global fit for scale

191 couples into the global seasonal deformation cycle due to hydrology. The ten-year

192 series JJ show hardly any improvement from corrections, anyplace. Scherneck et al.

193 (2003) have discussed in detail the low admittance of load series into the GPS

8

194   observations in the shorter daily version of the series (Johansson et al., 2002), using a

195   much larger set of stations.

196

197   The relative performance of the different hydrological models depends on the station

198   and on the time series, no clear pattern emerges. The correction for the Baltic level

199   ("bs") only works at Visby, which is situated in the middle of the Baltic Sea and also

200   near the coast. This is baffling as it is relatively large at all three stations. The poor

201   performance of the atmospheric correction ("aplo") may be in part related to the fact

202   that our correction is in CM frame while the other time series are approximately in the

203   CF frame. We thus neglect the geocenter motion (motion of the CM relative to CF)

204   due to the atmosphere, which is at the monthly timescale is of the order 3 mm (e.g.,

205   Feissel-Vernier et al., 2006) which in turn is as large as our atmospheric correction in

206   the CM frame. On the other hand, Tregoning and van Dam (2005) show that there are

207   several sites where the correction for atmospheric loading does not improve GPS

208   daily series even when both are in the same frame.

209

210   The largest reductions in the GPS residuals are 20–40%, for the MHp7 and MHp6

211   series. This is similar to the results by Tervo et al. (2006) but the difference is that

212   they reached best results by removing all the loading factors.

213   ***Influence of load corrections on trend determination***

214   All our stations are in the area of the Fennoscandian postglacial rebound and it is of

215   interest to see how the load corrections influence the trend determination from the

216   GPS time series. Obviously, the formal uncertainty of the trend fitted using least

217   squares will decrease in the same way as the residual standard deviation in Tables 1,

218   2, and 3. But what about the trend itself? Table 4 gives the results of trend

9

219   determination for the three stations. There is the GPS time series name and the time

220   period for which the trend was computed, the trend from daily values and the trend

221   from monthly values. As could be expected, the values are quite similar, since the

222   same data set is used. The rest of the columns show the trends computed for the

223   different loading signals. The last three columns show the sum of the trends using

224   different hydrological models. The figures give the opposite number of the change in

225   the trend of the GPS time series, if it were corrected for the corresponding load(s).

226   Most of the trends are small as expected

227   [Table 4]

228   The hydrological models are not constructed for determination of hydrological long-

229   term trends but rather for the annual cycle and for short-term inter-annual phenomena.

230   They could perhaps be trusted only over a few years. However, we see that in Visby

231   and Mårtsbo, where the uncertain trends from the short 3-year GPS time series deviate

232   appreciably from the 10-year GPS trend, the inclusion of the hydrological load would

233   only make the discrepancy worse. On the contrary, the modelled loads with the

234   exception of the CPC seem near trend-free over the 10-year period.

Seasonal variation in the GPS and in the loading time series

236   As discussed in the Introduction, GPS time series often show seasonal variation; in

237   apparent positions load phenomena like hydrology are also seasonal in nature.

238   Inspection of Figure 2 shows a clear seasonal signal in the hydrological time series,

239   and in the Metsähovi GPS series. For better visualization, we stack the GPS and load

240   time series for each site by averaging over each month separately. This simple method

241   has the advantage that no functional form (e.g. sinusoidal) is assumed for the

242   phenomena. The results are depicted in Figure 3. It shows the total load effect (in

10

243   which hydrology is represented by WGHM) and the three different GPS time series

244   for each station,

245   [Figure 3]

246   First note is that the load stacks are very similar at all stations and over both 10 and 3

247   years. In Metsähovi all time series are stacked over 10 years. The phases of the GPS

248   stack agree and are rather close to the phases of the load stack. The GPS amplitudes

249   are 40–80% of the load amplitude. JJ and MHp7 are near-identical as previously

250   noted. For Mårtsbo and Visby we use load stacks over 3 years and 10 years. GPS

251   stacks MHp6 and MHp7 are over 3 years and JJ over 3 and over 10 years. At Mårtsbo

252   the 3-year GPS stacks agree quite well. The amplitude of the JJ solution is not as clear

253   as for MHp6 and MHp7 but they all agree with the load. The 10-year JJ stack deviates

254   considerably from the load and shows only a very subdued annual cycle. At Visby,

255   the (3-year) MHp6 and MHp7 reproduce the phases of the load stack but have about

256   70 percent of its amplitude. The 3-year JJ stack is bimodal due to the data of the

257   winter 2006. The 10-year JJ stack does not show any seasonal pattern at all.

258

259   While at some stations the similarity of the annual cycle from GPS and from the load

260   models is obvious, it should be remembered that even at them the GPS seasonal

261   component explains only a part of the variation in the monthly GPS time series. E.g.

262   at Metsähovi subtracting the monthly means from the MHp6, MHp7, and JJ time

263   series decreases their standard deviation by 24, 11, and 5 percent, respectively. For the

264   3-year series at Mårtsbo the figures are 39, 5, and 5 percent. At Visby we have 13, –

265   18 and –18 percent, i.e. partly a deterioration. This is because we have taken into

266   account that in eliminating the monthly means the degrees of freedom decrease by 11.

11

267 **Conclusions and outlook**

268 We have studied the effect of the atmospheric pressure loading, the effect of the non-

269 tidal Baltic Sea loading and the effect of continental water loading at seven GPS

270 stations in Fennoscandia. Despite this being a limited region, the loading signals are

271 far from identical: the Baltic loading is limited to the vicinity of the sea and across the

272 region differences appear also in the continental water loading. At three sites close to

273 the Baltic the loading time series were compared with apparent vertical movements

274 derived from GPS. Removing the computed loading from the GPS time series reduce

275 the standard deviation, but not for all series nor for all combinations of loads. The

276 maximum reduction was found to be 23% at Metsähovi, 43% at Mårtsbo and 34% at

277 Visby. This is of the same size as in our previous results (Tervo et al., 2006).

278

279 The three GPS time series studied use the same processing strategy but different

280 alignment to the reference frame. This is reflected in their relationship to the load time

281 series. The MHp6 does not use a scale parameter in the alignment and after correcting

282 for the loads performs better than the MHp7 that does. The 10-year JJ and MHp7

283 series are not significantly improved by the loading corrections on any of the stations,

284 but the corresponding 3-year series at Mårtsbo are. For control we computed the 3-

285 year series at Metsähovi and found the same results (not shown) as at Mårtsbo. This

286 could be related to the piecewise transformations used in the alignment to the frame.

287

288 The three time series of hydrological loads differ appreciably but the GPS series do

289 not show clear preference for any of them. Obviously, there is considerable

290 uncertainty the models involved. No such uncertainty should appear in our Baltic load

12

291   model and therefore it is baffling that it does not perform better for the GPS. We will

292   improve the atmospheric load series by including the corresponding geocentre motion.

293

294   At the three stations analyzed, removing the seasonal variation decreases the standard

295   deviation of the monthly GPS solutions by maximally 40 percent. The seasonal

296   variation in GPS tends to underestimate the seasonal variation in modelled load.

297

303

304   References

305   Agnew, D.C., 1997. NLOADF: A program for computing ocean-tide loading, J.

306   Geophys. Res., 102, 5109-5110.

307

308   Blewitt, G., Lavallée, D., Clark P., Nurutdinov K, 2001. A new global mode of Earth

309   deformation: Seasonal cycle detected, Science, 294, 2342– 2345.

310

311   Clarke, P. J., Lavallée, D., Blewitt, G., van Dam, T,. Wahr J. M., 2005. Effect of

312   gravitational consistency and mass conservation on seasonal surface mass loading

313   models, Geophys. Res. Lett., 32, L08306, doi:10.1029/2005GL022441

314

13

315   Döll, P., Kaspar, F., Lehner, B., 2003. A global hydrological model for deriving water

316   availability indicators: model tuning and validation. J. Hydrol. 270, 105-134.

317

318   Dong, D., Fang P., Bock Y., Cheng M. K., Miyazaki S., 2002. Anatomy of apparent

319   seasonal variations from GPS-derived site position time series, J. Geophys. Res.,

320   107(B4), 2075, doi:10.1029/2001JB000573.

321

322   Dong, D., Yunck, T., Heflin M., 2003. Origin of the International Terrestrial

323   Reference Frame, J. Geophys. Res., 108(B4), 2200, doi:10.1029/2002JB002035

324

325   Fan, Y., van den Dool H., 2004. Climate Prediction Center global monthly soil

326   moisture data set at 0.5° resolution for 1948 to present, J. Geophys. Res., 109,

327   D10102, doi:10.1029/2003JD004345.

328

329   Farrell, W.E., 1972. Deformation of the Earth by surface loads. Rev. Geophys. Space

330   Phys. 10, 761–797.

331

332   Feissel-Vernier, M., Le Bail, K., Berio, P., Coulot, D., Valette, J. 2006. Geocenter

333   motion measured with DORIS and SLR and predicted by geophysical models,,

334   Journal of Geodesy, 80, 637-648, DOI 10.1007/s00190-006-0079-z

335

336   Johansson, J.M., Davis J.L., Scherneck H.-G., Milne G.A., Vermeer M., Mitrovica

337   J.X., Bennett R.A., Elgered G., Elósegui P., Koivula H., Poutanen M., Rönnäng B.O.,

338   Shapiro I.I., 2002. Continuous GPS measurements of postglacial adjustment in

14

339   Fennoscandia, 1. Geodetic Results, J. Geophys. Res., Vol. 107, No. B8, DOI

340   10.1029/2001JB000400.

341

342   King, M. A., Watson, C. S., Penna, N. T., Clarke P. J., 2008. Subdaily signals in GPS

343   observations and their effect at semiannual and annual periods, Geophys. Res. Lett.,

344   35, L03302, doi:10.1029/2007GL032252.

345

346   Milly, P. C. D., Shmakin A. B., 2002. Global modeling of land water and energy

347   balances. part I: The Land Dynamics (LaD) model, J. Hydrometeorol., 3, 283– 299.

348

349   Munekane, H., Kuroishi, Y., Hatanaka Y. Yarai H., 2008. Spurious annual vertical

350   deformations over Japan due to mismodelling of tropospheric delays, Geophys. J. Int.

351   (2008) 175, 831–836 doi: 10.1111/j.1365-246X.2008.03980.x

352

353   Penna, N. T., Stewart M. P., 2003. Aliased tidal signatures in continuous GPS height

354   time series, Geophysical Research Letters, 30(23), 2184, doi:10.1029/2003GL018828.

355

356   Penna, N., King M., Stewart M., 2007. GPS height time series: Short period origins of

357   spurious long period signals, J. Geophys. Res., 112, B02402,

358   doi:10.1029/2005JB004047.

359

360   Petrov, L. Boy J.-P., 2004. Study of the atmospheric pressure loading signal in VLBI

361   observations, Journal of Geophysical Research, 10.1029/2003JB002500, Vol. 109,

362   No. B03405.

363

364   R Development Core Team, 2006. R: A language and environment for statistical

365   computing, R Foundation for Statistical Computing, Vienna, Austria. ISBN 3-

366   900051-07-0, URL http://www.R-project.org.

367

368   Ray, J., Altamimi, Z., Collilieux, X., van Dam, T., 2008. Anomalous harmonics in the

369   spectra of GPS position estimates. GPS Solutions 12, 55–64.

370

371   Scherneck H.-G., Johansson J.M., Koivula H., van Dam, T., Davis J.L., 2003. Vertical

372   crustal motion observed in the BIFROST project. Journal of Geodynamics, Vol 35,

373   No.4-5, pp.425-441

374

375   Smith, W.H.F. Wessel, P., 1990. Gridding with continuous curvature splines in

376   tension, Geophysics, 55, 293–305.

377   .

378   Stewart, M. P., Penna N. T., Lichti D. D., 2005. Investigating the propagation

379   mechanism of unmodelled systematic errors on coordinate time series estimated using

380   least squares, J. Geod., 79, 479 – 489, doi:10.1007/s00190-005-0478-6.

381

382   Takiguchi, H., Otsubo, T., Fukuda, Y., 2006. Mass-redistribution-induced crustal

383   deformation of global satellite laser ranging stations due to non-tidal ocean and land

384   water circulation, Earth, Planets and Space, Volume 58, p. e13-e16.

385

386   Tervo M., Virtanen H., Bilker-Koivula M., 2006. Environmental loading effects on

387   GPS time series, Bull. d'Inf. Marées Terr. 142: 11407 – 11416.

388

16

389   Tregoning P., van Dam T., Atmospheric pressure loading corrections applied to GPS

390   data at the observation level, Geophys. Res. Lett., 32, L22310,

391   doi:10.1029/2005GL024104, 2005.

392

393   van Dam, T., Blewitt G., Heflin M.B., 1994. Atmospheric pressure loading effects on

394   GPS coordinate determinations, J. Geophys. Res., 99, 23939-23950.

395

396   van Dam, T., Wahr J., Milly P.C.D., Shmakin A.B., Blewitt G., Lavallée D., Larson

397   K.M., 2001. Crustal displacements due to continental water loading, Geophysical

398   Research Letters, 28, 651-654.

399

400   van Dam, T., Wahr J., Lavallée D., 2007. A comparison of annual vertical crustal

401   displacements from GPS and Gravity Recovery and Climate Experiment (GRACE)

402   over Europe, J. Geophys. Res., 112, B03404, doi:10.1029/2006JB004335.

403

404   Virtanen, J., Mäkinen, J., Koivula-Bilker, M., Virtanen, H., Nordman, M., Kangas, A.,

405   Johansson, M., Shum, C.K., Lee, H., Wang L., Thomas, M., 2008. Baltic sea mass

406   variations from GRACE: comparison with in situ and modelled sea level heights.

407   Presented at the IAG International Symposium "Gravity, Geoid and Earth

408   Observation 2008" GGEO2008, Chania, Crete, 23–27 June 2008. In press.

409

410   Williams, S. D. P., Bock Y., Fang P., Jamason P., Nikolaidis R. M., Prawirodirdjo L.,

411   Miller M., Johnson D. J., 2004. Error analysis of continuous GPS position time series,

412   J. Geophys. Res., 109, B03412, doi:10.1029/2003JB002741.

413

17

414   Wessel, P. Smith, W. H. F., 1998. New, improved version of Generic Mapping Tools

415   released, EOS Trans. Amer. Geophys. U., 79, 579

416

417   Woodworth, P., Player R., 2003. The Permanent service for mean seal level: an

418   update to the 21st century. J. of Coas. Res. 19(2), pp.287-295.

419

420

18

Figure and table captions

Figure 1. a) Loading caused by the Baltic Sea in March 2006 and the positions of the GPS stations. The scale is in millimetres. b) The GPS time series of all the stations, scale is in millimetres. TROM=Tromsö, KIRU=Kiruna, MART=Mårtsbo, METS=Metsähovi, VISB=Visby, BORA= Borås, ONSA=Onsala. Solid black line = JJ, gray line = MHp6, dashed black line = MHp7.The peaks in Kiruna ja Tromsö time series are likely due to snow accumulation on top of the antenna.

Figure 2. Time series. a) Metsähovi b) difference Kiruna – Metsähovi (distance 880 km) c) difference Mårtsbo – Metsähovi (distance 410 km) d) difference Onsala – Metsähovi (distance 790 km). The top panel (gps) is the GPS time series (or the difference) after trend removal: solid black line = JJ, gray line = MHp6, dashed black line = MHp7. The second panel from top (bs) is the Baltic Sea loading and the third panel (ap) the atmospheric pressure loading. The fourth panel (cw) shows three different continental water model loads: solid black line = CPC, gray line = WGHM, dashed black line = LadWorld. The fifth panel shows the sum of the loads i.e. panels 2, 3 and 4. The bottom panel (resid) shows the GPS time series residual after the loading time series are subtracted. The WGHM was used for water load. The different lines are the same as for the top panel. The peaks in the Kiruna GPS time series are due to snow accumulation on top of the antenna. The scale is in millimetres.

Figure 3. Stacked time series for stations Metsähovi, Mårtsbo and Visby. The monthly mean for the whole time series has been computed and plotted. The circles show the sum of the loading factors, the triangles show the JJ time series and the grey symbols

19

445   show the MH time series, plusses the 6-parameter transformation and crosses the 7-

446   parameter transformation. The dashed line is for 10-year time series of JJ and solid

447   line for 3-year in Mårtsbo and Visby.

448

449   Table 1. The results for station Visby, standard deviations in mm of the different time

450   series and their reduction with respect to the original time series. MH p6 = MH time

451   series with 6-parameter transformation, MH p7 = the same, but with 7 parameters, JJ

452   = BIFROST time series, JJS = JJ time series for 3 years, red % = reduction percentage

453   of the standard deviation, gps = GPS time series after trend removal, aplo =

454   atmospheric pressure loading, bs = Baltic Sea loading, wghm = continental water

455   loading from model WGHM, cpc = continental water loading from model CPC, ladw

456   = continental water loading from model LadWorld. The standard deviations of the

457   load time series (aplo, bs, wghm, cpc, ladw) are 2.73, 2.01, 3.91, 2.01, 0.80 mm (10

458   years) and 2.81, 2.19, 3.77, 1.70, 0.83 mm (3 years).

459

460   Table 2. The results for the station Mårtsbo. The abbreviations are the same as in

461   Table 1. The standards deviations of the load time series (aplo, bs, wghm, cpc, ladw)

462   are 2.72, 1.24, 4.23, 2.18, 1.68 mm (10 years) and 2.68, 1.34, 3.96, 1.82, 1.68 (3

463   years).

464

465   Table 3. The results for the station Metsähovi. The abbreviations are the same as in

466   Table 1. The standards deviations of the load time series (aplo, bs, wghm, cpc, ladw)

467   are 3.07, 1.38, 4.75, 2.27, 2.35 mm.

468

20

469   Table 4. The determined trends (mm/year) from different time series. The first

470   column gives the name of the GPS time series, MHp6 = MH time series with 6-

471   parameter transformation, MHp7 = the same, but with 7 parameters, JJ = BIFROST

472   time series, and their length (10 or 3 years). gps/d = trend determined from daily GPS

473   time series, gps /m = trend from the monthly time series, aplo = atmospheric pressure

474   loading, bs = Baltic Sea loading, wghm = continental water loading from model

475   WGHM, cpc = continental water loading from model CPC, ladw = continental water

476   loading from model LadWorld, sum (A) = the trend of the sum of the loadings using

477   different water models A.

478

21

478
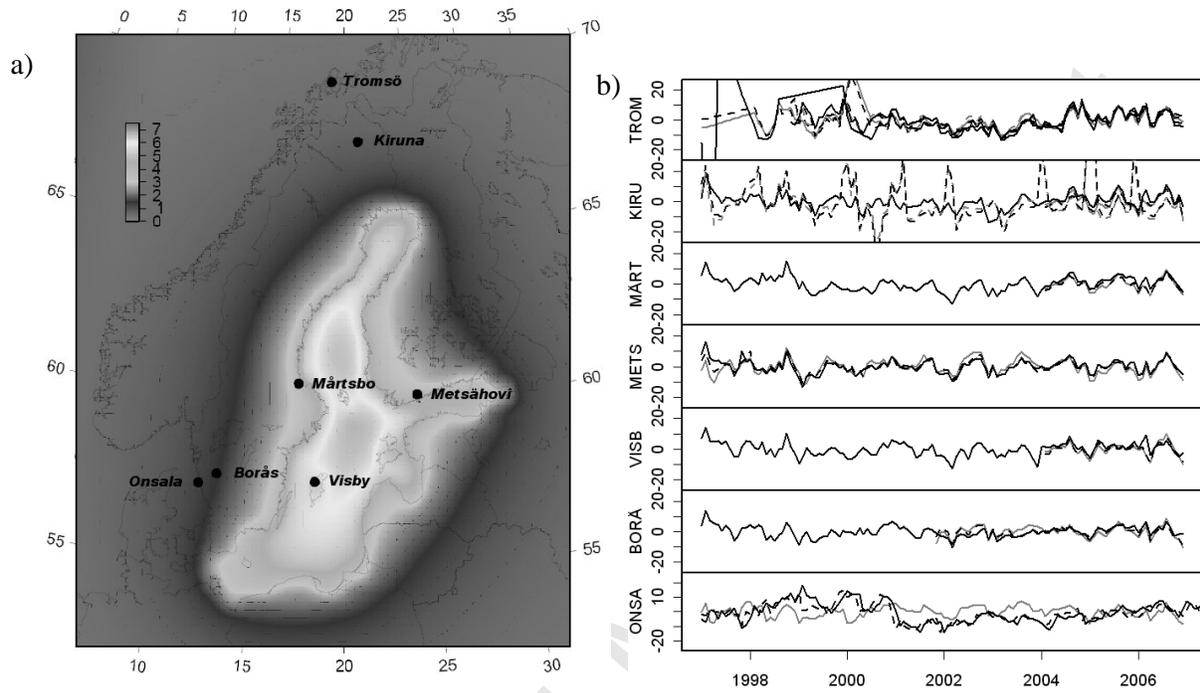
Figures

480
481 Figure 1. a) Station positions and loading in millimetres for March 2006. b) GPS time
482 series.
483
484

22

484

485 a)
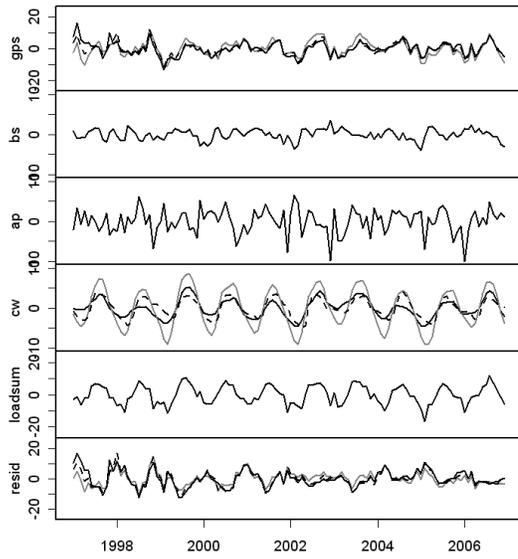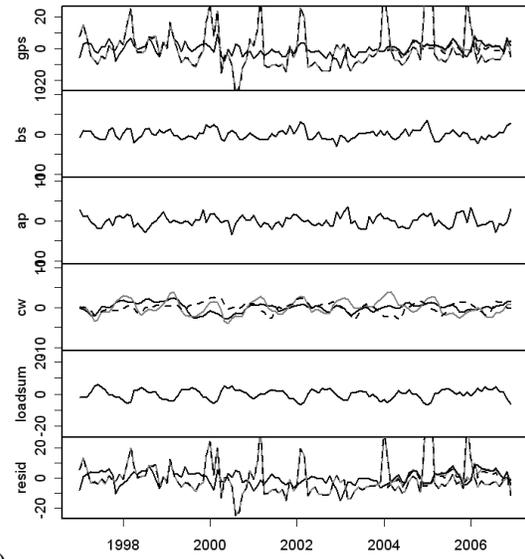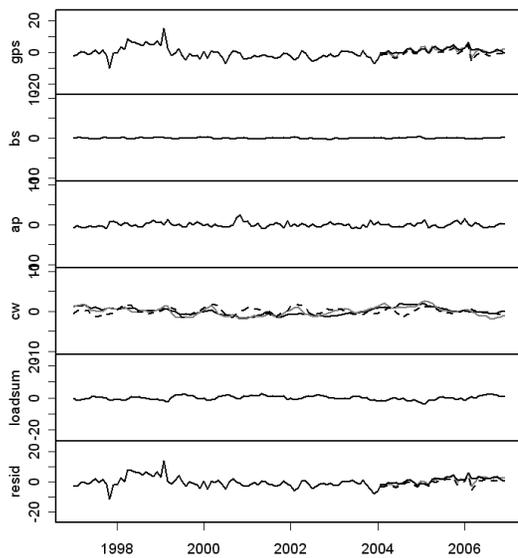
c)   d)
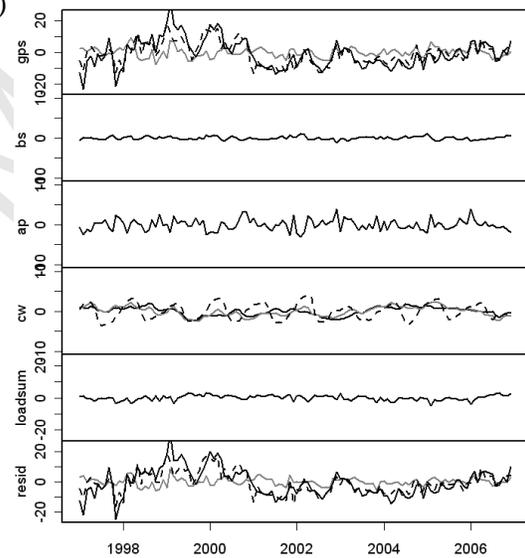
486

487

488 Figure 2. Time series. a) Metsähovi b) difference Kiruna – Metsähovi c) difference
489 Mårtsbo – Metsähovi d) difference Onsala – Metsähovi.
490

23

490

491

492
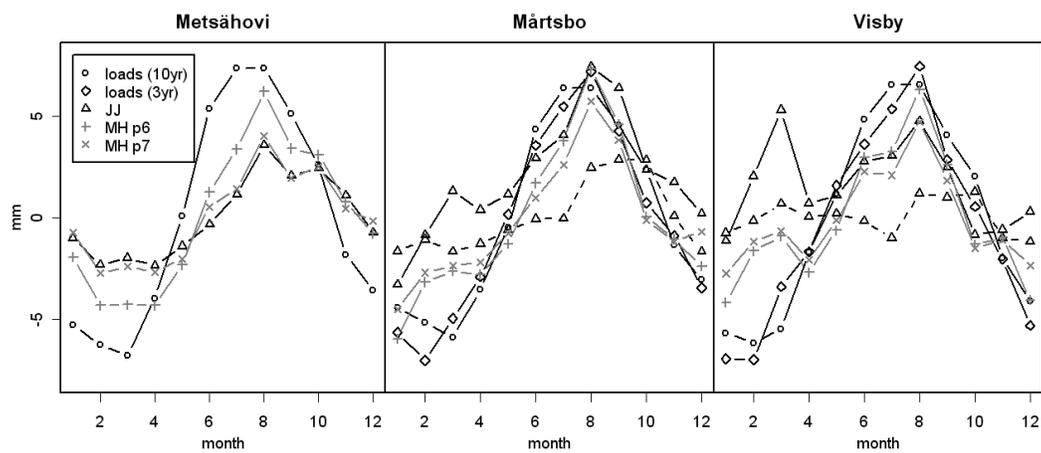
493   Figure 3. Stacked time series for all three stations.

494

495

24

495

Tables

497

498 Table 1. Results for Visby

499

VISBY	MHp6	red %	MHp7	red %	JJS (3-yr)	red %	JJ(10-yr)	red %
gps	4.22	0.0	3.61	0.0	3.22	0.0	4.38	0.0
- aplo	4.66	10.4	4.33	20.0	4.02	24.7	5.38	22.6
- bs	3.96	-6.3	3.34	-7.4	2.49	-22.7	4.05	-7.7
- wghm	3.47	-17.9	3.62	0.5	4.31	33.6	5.53	26.1
- cpc	3.28	-22.3	3.00	-16.9	3.13	-2.8	4.41	0.5
- ladw	3.85	-8.9	3.36	-6.8	3.10	-3.9	4.47	2.0
- aplo-bs	4.18	-1.1	3.85	6.6	3.14	-2.5	4.74	8.2
- aplo-wghm	4.60	9.0	4.91	36.1	5.44	68.7	6.54	49.2
- bs-wghm	2.78	-34.1	3.03	-16.0	3.50	8.7	5.36	22.2
- aplo-bs-wghm	3.85	-8.9	4.25	17.8	4.60	42.9	6.11	39.4
- aplo-bs-cpc	3.64	-13.7	3.70	2.4	3.50	8.5	4.95	12.9
- aplo-bs-ladw	3.81	-9.9	3.63	0.6	3.03	-6.0	4.82	9.9

500
501
502

25

502

503   Table 2. Results for Mårtsbo

504

MÅRTSBO	MHp6	red %	MHp7	red %	JJS (3-yr)	red %	JJ(10-yr)	red %
gps	4.05	0.0	3.29	0.0	3.41	0.0	4.65	0.0
- aplo	4.08	0.8	3.53	7.3	3.76	10.2	5.31	14.3
- bs	4.21	4.1	3.51	6.6	3.42	0.2	4.68	0.8
- wghm	2.29	-43.4	2.48	-24.5	2.61	-23.6	5.10	9.9
- cpc	2.58	-36.2	2.15	-34.8	2.35	-31.1	4.31	-7.3
- ladw	2.94	-27.3	2.40	-27.2	2.66	-22.1	4.61	-0.8
- aplo-bs	3.88	-4.1	3.32	0.8	3.35	-1.7	5.01	7.9
- aplo-wghm	3.22	-20.4	3.56	8.2	3.76	10.4	5.77	24.2
- bs-wghm	2.29	-43.3	2.51	-23.8	2.34	-31.3	5.19	11.6
- aplo-bs-wghm	2.73	-32.6	3.14	-4.7	3.15	-7.7	5.54	19.2
- aplo-bs-cpc	2.89	-28.7	2.79	-15.4	2.85	-16.5	4.79	3.1
- aplo-bs-ladw	2.89	-28.7	2.63	-20.1	2.77	-18.8	4.99	7.4

505
506
507

507   Table 3. Results for Metsähovi

508

METSÄHOVI	MHp6	red %	MHp7	red %	JJ	red %
gps	4.98	0.0	4.05	0.0	4.47	0.0
- aplo	5.50	10.6	4.76	17.4	5.15	15.1
- bs	5.01	0.6	4.19	3.4	4.58	2.4
- wghm	3.82	-23.2	4.45	10.0	4.95	10.7
- cpc	3.97	-20.3	3.65	-9.8	4.11	-8.1
- ladw	3.94	-20.8	3.68	-9.1	4.24	-5.2
- aplo-bs	5.17	3.8	4.46	10.0	4.85	8.5
- aplo-wghm	4.69	-5.7	5.28	30.5	5.74	28.2
- bs-wghm	4.01	-19.4	4.71	16.2	5.17	15.5
- aplo-bs-wghm	4.43	-11.1	5.13	26.7	5.58	24.8
- aplo-bs-cpc	4.40	-11.6	4.30	6.1	4.70	5.1
- aplo-bs-ladw	4.22	-15.2	4.17	2.9	4.68	4.7

509

510

511

27

511

512   Table 4. Trend determination

	mm/year	gps/d	gps/m	aplo	bs	wghm	cpc	ladw	sum (wghm)	sum (cpc)	sum (ladw)
METS	MHp6 (10yr)	5.48	5.43	-0.19	0.04	0.20	0.42	0.08	0.04	0.27	-0.07
	MHp7 (10yr)	5.61	5.58								
	JJ (10 yr)	5.48	5.45								
MART	MHp6 (3yr)	7.51	7.19	-0.17	0.06	0.58	0.80	0.27	0.48	0.70	0.17
	MHp7 (3yr)	7.85	7.68								
	JJ (3yr)	8.20	7.82								
	JJ (10 yr)	8.12	7.90	-0.17	0.03	0.17	0.50	0.01	0.03	0.36	-0.13
VISB	MHp6 (3yr)	2.03	1.46	-0.23	0.05	0.96	1.08	0.18	0.78	0.89	0.00
	MHp7 (3yr)	2.38	1.95								
	JJ (3yr)	3.33	3.14								
	JJ (10 yr)	3.56	3.78	-0.16	0.05	0.10	0.43	0.04	-0.01	0.31	-0.08

513
514

28